BIOE 476: Tissue Engineering, Fall 2018

Homework 3- due Tuesday, October 16th (in class)

- Read the following article: DeMuth et al. Polymer multilayer tattooing for enhanced DNA vaccination. *Nature Materials* (2013), and answer the following questions (a-j). For some questions, you may need to look into referenced papers or outside material for additional information.
  http://www.nature.com/nmat/journal/vaop/ncurrent/full/nmat3550.html

3 points each, 30 points total

a) Polyelectrolyte multilayers (PEMs) are films of alternately charge polymers. What are the positively charged polymers used in this work? What are the negatively charged polymers used in this work?

b) What is the composition of the 'release layer'? What purpose does this layer serve, and what are the key characteristics of this layer?

c) What are the 2 signals that can be detected using Cy5 pLUC and what do they measure?

d) Why is the co-localization of pLUC and poly(I:C) with MHC-II+ cells a positive finding (i.e. a good thing)?

e) What is poly(I:C), and why is it co-delivered with plasmid DNA in these studies?

f) What benefit does the poly-2 PBAE formulation exhibit compared to the poly-1 PBAE formulation?

g) What do the in vivo luminol experiments (Figure 4b) demonstrate?

h) What advantage does the described technology have compared to in vivo electroporation?

i) What advantage does the described technology have compared to intradermal injection of polymer-pDNA complexes?

j) What are 2 advantages that the described technology has compared to needle-based administration of a liquid vaccine?

nature materials

ARTICLES

PUBLISHED ONLINE: 27 JANUARY 2013 | DOI: 10.1038/NMAT3550

Polymer multilayer tattooing for enhanced DNA vaccination

Peter C. DeMuth[1], Younjin Min[2], Bonnie Huang[1], Joshua A. Kramer[3], Andrew D. Miller[3], Dan H. Barouch[4,5], Paula T. Hammond[2,6,7]* and Darrell J. Irvine[1,5,6,7,8,9]*

DNA vaccines have many potential benefits but have failed to generate robust immune responses in humans. Recently, methods such as *in vivo* electroporation have demonstrated improved performance, but an optimal strategy for safe, reproducible, and pain-free DNA vaccination remains elusive. Here we report an approach for rapid implantation of vaccine-loaded polymer films carrying DNA, immune-stimulatory RNA, and biodegradable polycations into the immune-cell-rich epidermis, using microneedles coated with releasable polyelectrolyte multilayers. Films transferred into the skin following brief microneedle application promoted local transfection and controlled the persistence of DNA and adjuvants in the skin from days to weeks, with kinetics determined by the film composition. These 'multilayer tattoo' DNA vaccines induced immune responses against a model HIV antigen comparable to electroporation in mice, enhanced memory T-cell generation, and elicited 140-fold higher gene expression in non-human primate skin than intradermal DNA injection, indicating the potential of this strategy for enhancing DNA vaccination.

DNA vaccines have been intensively studied because of potential advantages such as ease of good manufacturing practice production, lack of anti-vector immunity, and the capability to promote both cellular and humoral immune responses[1,2]. However, plasmid DNA (pDNA) immunization has shown poor efficacy in non-human primates and human trials[1,3], and the most promising methods for increasing the potency of these vaccines have employed complicated methods such as *in vivo* electroporation that are not attractive for widespread prophylactic vaccination[4]. Parallel to the technical challenges of DNA vaccination, traditional needle-based administration of vaccines has a number of disadvantages: liquid vaccine formulations typically require refrigeration, which raises the cost and complexity of global distribution (the 'cold chain')[5], administration requires trained personnel, and safety is hampered by needle re-use and needle-based injuries[6]. These issues become particularly acute for vaccine distribution in the developing world[6–8].

We hypothesized that DNA vaccine delivery would be substantially enhanced by an approach that could simultaneously target DNA to tissues rich in immune-response-governing dendritic cells, promote sustained transfection without toxicity, and provide supporting inflammatory cues to enhance the induction of a potent immune response. Moreover, vaccines have been shown to vary widely in potency, depending on the kinetics of both antigen and adjuvant exposure, with optimal immunity often stimulated by the persistence of antigen and inflammatory signals for up to one week[9–12]. To meet these design goals, we developed a strategy using microneedles to rapidly implant into the skin biodegradable polymer films, which continuously release DNA polyplexes and adjuvant molecules in this immunologically competent tissue over a tunable and sustained period of time. We show that skin-implanted vaccine multilayers allow control over the physical and functional persistence of inflammatory adjuvants and pDNA, efficiently transfecting cells in murine skin and eliciting cellular and humoral immune responses comparable to or exceeding *in vivo* electroporation of pDNA, one of the most promising current technologies for DNA vaccine delivery[4]. We have termed this approach of implanting persistent polymer films into the skin 'multilayer tattooing', by analogy to conventional tattooing, where persisting inks are deposited in the skin. These multilayer vaccine formulations allow for dry-state storage of coated microneedle patches at room temperature for weeks without loss of activity, an important advantage for decreasing costs and improving vaccine availability in remote areas. Further, when applied to viable macaque skin *ex vivo*, multilayer tattooing elicited 140-fold greater gene expression compared to naked DNA injection. Thus, this polymer film tattooing approach may offer a route to efficacious DNA vaccines via a pain-free and self-administrable dry skin-patch platform.

We first set out to create implantable vaccine coatings using polyelectrolyte multilayers[13,14] (PEMs, Fig. 1a), nanostructured films formed by iterative adsorption of alternately charged polymers, which embed large weight-fractions of biologic cargos (for example, DNA, up to 40% of total film mass)[15], stabilize embedded molecules in the dried state[16,17], and exhibit release kinetics predetermined by the film architecture/composition. We hypothesized that rapid multilayer transfer from coated microneedles into the epidermis could be achieved via an underlying polymer film designed to instantly dissolve when

[1]Department of Biological Engineering, Massachusetts Institute of Technology (MIT), Cambridge, Massachusetts 02139, USA, [2]Department of Chemical Engineering, MIT, Cambridge, Massachusetts 02139, USA, [3]New England Primate Research Center, Harvard Medical School, Southborough, Massachusetts 01772, USA, [4]Division of Vaccine Research, Beth Israel Deaconess Medical Center, Harvard Medical School, Boston, Massachusetts 02215, USA, [5]Ragon Institute of MGH, MIT, and Harvard, Charlestown, Massachusetts 02129, USA, [6]Institute for Soldier Nanotechnologies, MIT, Cambridge, Massachusetts 02139, USA, [7]Koch Institute for Integrative Cancer Research, MIT, Cambridge, Massachusetts 02139, USA, [8]Department of Materials Science and Engineering, MIT, Cambridge, Massachusetts 02139, USA, [9]Howard Hughes Medical Institute, Chevy Chase, Maryland 20815, USA.
*e-mail: hammond@mit.edu; djirvine@mit.edu.

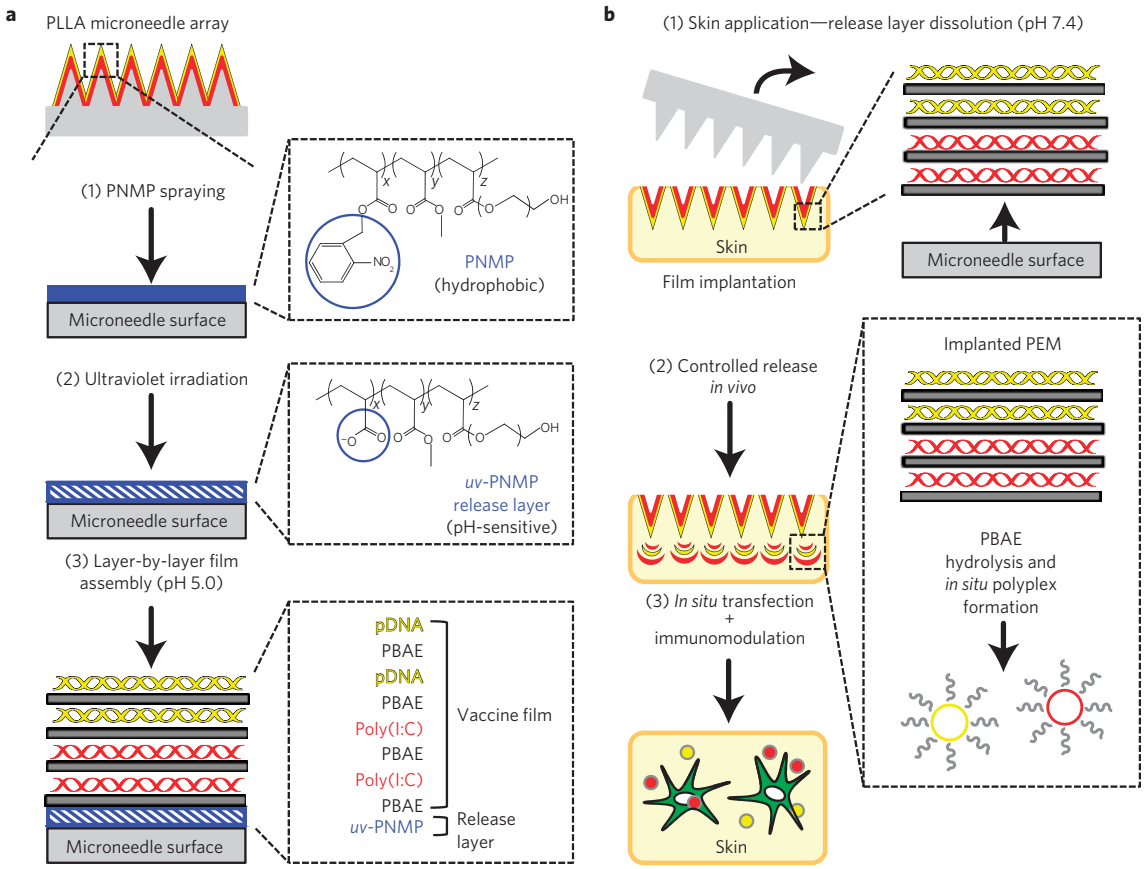

Figure 1 | Design of quick-release vaccine-loaded microneedle coatings. a, Schematic view of release-layer-mediated multilayer tattooing strategy using coated microneedles: (1) PLLA microneedles are coated with PNMP release-layer films through spray deposition; (2) ultraviolet irradiation imparts pH-sensitive aqueous solubility to the PNMP film, forming a *uv*-PNMP 'release-layer'; (3) Overlying multilayer films containing nucleic acids are constructed using LbL deposition at pH 5.0. **b**, Mechanism of action for multilayer tattooing: (1) Microneedle application to skin and exposure to interstitial fluid gives rapid release-layer dissolution, mediating overlying film delamination and retention in skin following microneedle removal; (2) Implanted films provide sustained release of nucleic acids through hydrolytic PBAE degradation and release of *in situ*-formed PBAE/nucleic acid polyplexes; (3) released polyplexes mediate local transfection and immune modulation in the tissue.

microneedles are applied to the skin (Fig. 1b), allowing the kinetics of DNA/adjuvant release in the tissue to be tailored separately from the time required for a microneedle patch to be kept on the skin. To create such releasable vaccine coatings, we employed a photo-sensitive and pH-responsive polymer, poly(*o*-nitrobenzyl -methacrylate-*co*-methyl-methacrylate-*co*-poly(ethylene-glycol)-methacrylate) (PNMP), for the release-layer. PNMP is initially organic-soluble, but on brief exposure to ultraviolet, cleavage of the *o*-nitrobenzyl groups converts the polymer to a weak polyelectrolyte (*uv*-PNMP) soluble in water above pH ~6.5 (ref. 18). As shown below, this photo-switchable solubility provided the means to prove that PEM film implantation depended on PNMP release-layer dissolution.

Skin patches were fabricated by melt-moulding poly(L-lactide) (PLLA) on poly(dimethylsiloxane) (PDMS) moulds to obtain arrays of microneedles, each 250 μm in diameter at their base and 650 μm in height (Supplementary Fig. S1)[19]. Biotinylated-PNMP (bPNMP, Supplementary Fig. S2a) films were coated on microneedles by spray deposition[20] from 1,4-dioxane solutions, exposed to ultraviolet to trigger the photochemical transition in the film, and then stained with fluorescent streptavidin (SAv) to permit visualization of the release-layer by microscopy. Next, LbL deposition was used to construct an overlying PEM film composed of Cy5-labelled pDNA encoding luciferase (Cy5-pLUC) and the transfection agent poly-1, a biodegradable poly(β-amino-ester) (PBAE, Supplementary Fig. S2b)[19,21]. PEM films were initiated by depositing 20 bilayers of protamine-sulphate (PS) and poly(4-styrene-sulphonate) (SPS) to provide a uniform charge density, followed by iterative adsorption of poly-1 and Cy5-pLUC (Fig. 2a). Profilometry measurements performed on PEMs constructed in parallel on Si substrates showed linear multilayer growth with increasing deposition cycles, as previously reported for (PBAE/pDNA) films (Fig. 2b)[19,21]. Confocal imaging of microneedles coated with composite (*uv*-bPNMP)(PS/SPS)$_{20}$(poly-1/Cy5-pLUC)$_{35}$ PEM films showed conformal co-localized fluorescence from SAv-labelled *uv*-bPNMP and Cy5-pLUC over the surface of each PLLA microneedle (Fig. 2c). (Individual *uv*-bPNMP and PEM films were too thin to resolve as distinct layers.) When analysed at sequential stages of PEM film deposition, the mean total SAv-bPNMP fluorescence signal from single microneedles was stable, but Cy5-pLUC fluorescence linearly increased with increasing rounds of bilayer deposition, confirming linear film growth on microneedles (Fig. 2d). Measurement of DNA recovered from microneedle coatings disrupted by treatment with sodium chloride showed ~4.2 μg DNA deposited per bilayer per cm^2 of the microneedle array (Fig. 2d). Sequential assembly of PEM films comprising layers of (poly-1/poly(I:C)) followed by layers of (poly-1/pLUC) generated microneedles coated with complete

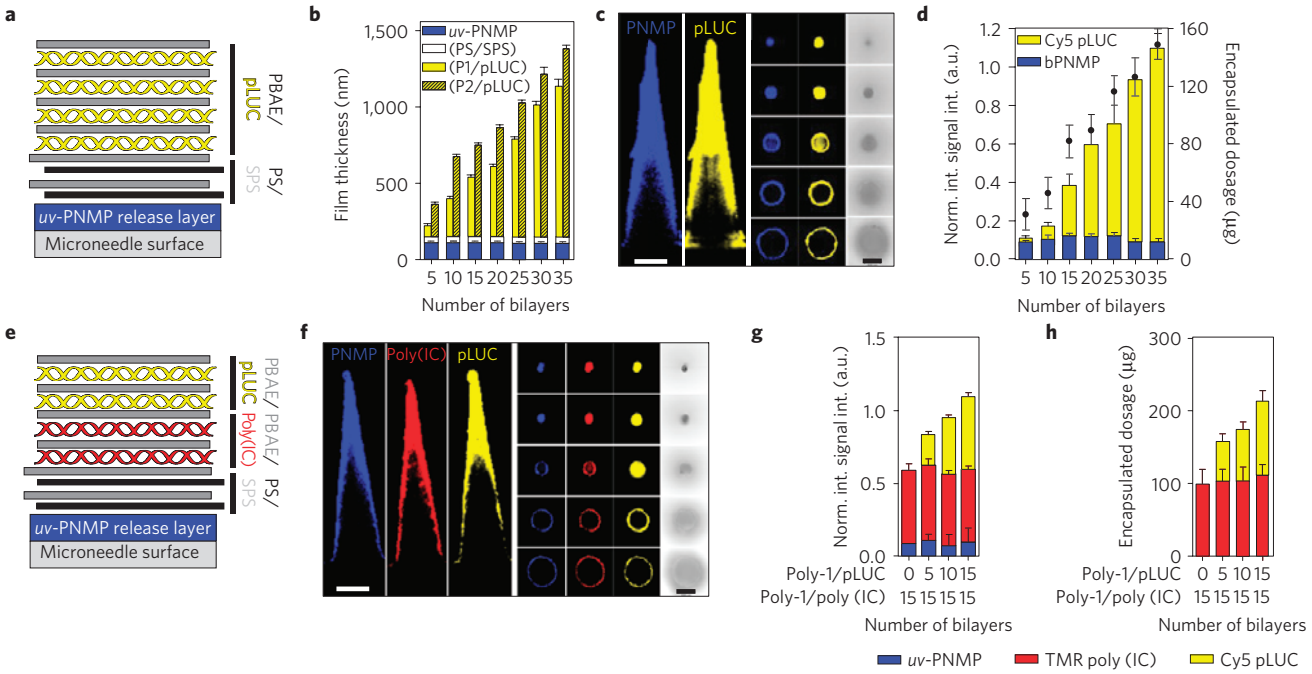

Figure 2 | LbL assembly of microneedle coatings carrying DNA, immunostimulatory RNA, and transfection agents. a, Film architecture for $(uv\text{-PNMP})(PS/SPS)_n(PBAE/pLUC)_n$ multilayers. **b**, Growth of $(poly\text{-}1/pLUC)_n$ and $(poly\text{-}2/pLUC)_n$ multilayers assembled onto $(uv\text{-PNMP})(PS/SPS)_{20}$ films on silicon substrates as a function of the number of deposited (PBAE/pLUC) bilayers as measured by surface profilometry. Data represent the mean ± s.e.m., $n = 8$. **c**, Representative confocal images of PLLA microneedles coated with $(SAv488\text{-}bPNMP)(PS/SPS)_{20}(poly\text{-}1/Cy5\text{-}pLUC)_{35}$ films (left, transverse optical sections; right, lateral sections, 100 μm *z*-intervals, scale bars, 200 μm; blue, Sav488-*uv*-bPNMP; yellow, Cy5-pLUC). **d**, Quantification of Cy5-pLUC and Sav488-bPNMP incorporated into $(SAv488\text{-}bPNMP)(PS/SPS)_{20}(poly\text{-}1/Cy5\text{-}pLUC)_n$ films on microneedles through confocal fluorescence intensity analysis (left axis, $n = 15$) and measurement of total DNA recovered from dissolved films (right axis, $n = 3$). Data represent the mean ± s.e.m. **e**, Film architecture for $(uv\text{-PNMP})(PS/SPS)_{20}(poly\text{-}1/pLUC)_n(poly\text{-}1/poly(I:C))_n$ multilayers. **f**, Representative confocal images of microneedles coated with $(SAv488\text{-}uv\text{-}bPNMP)(PS/SPS)_{20}(poly\text{-}1/TMR\text{-}poly(I:C))_{15}(poly\text{-}1/Cy5\text{-}pLUC)_{15}$ films (left, transverse sections; right, lateral sections, 100 μm *z*-intervals; scale, 200 μm; blue, Sav488-*uv*-bPNMP; yellow, Cy5-pLUC; red, TMR-poly(I:C)). **g**,**h**, Quantification of Cy5-pLUC, TMR-poly(I:C), and SAv488-bPNMP incorporated into $(SAv488\text{-}bPNMP)(PS/SPS)_{20}(poly\text{-}1/TMR\text{-}poly(I:C))_n(poly\text{-}1/Cy5\text{-}pLUC)_n$ films on microneedles through confocal fluorescence intensity analysis (**g**, $n = 15$) and measurement of total nucleic acids recovered from dissolved films (**h**, $n = 3$). Data represent the mean ± s.e.m.

vaccine multilayers containing pDNA, a transfection agent, and a strong adjuvant (Fig. 2e). These composite films showed conformal coating of both vaccine components (Fig. 2f) and linear growth of pLUC layers over poly(I:C) layers with increasing number of deposition cycles (Fig. 2g,h). Key to this process is that the DNA-containing PEM is never exposed to ultraviolet irradiation, thus avoiding any potential damage due to ultraviolet exposure.

Lack of toxicity/biocompatibility is critical for materials used in prophylactic vaccines, and the components of the microneedle system were chosen with biocompatibility in mind: polylactide, used as the microneedle base, is a bioresorbable polymer with a long history of clinical use in resorbable sutures and drug delivery devices. Although we chose to use (PS/SPS) 'base-layer' films for convenience in lab-scale studies, simplified film architectures composed of only PNMP and (PBAE/nucleic acids) could be deposited with linear growth per deposition cycle for 20 or more bilayers (data not shown). Previous studies have demonstrated the biocompatibility of both PNMP *in vitro*[18,22] and poly-1 and poly-2 polymers *in vitro* and *in vivo*[23–25]. Consistent with these data, we observed no apparent local toxicity in any of the mice treated throughout these studies.

To test PEM film release from microneedle arrays, dried composite (SAv-labelled *uv*-bPNMP)$(PS/SPS)_{20}(poly\text{-}1/Cy5\text{-}pLUC)_{35}$ coatings (referred to henceforth as PNMP/PEM films) on microneedles were immersed in pH 7.4 PBS for varying times *in vitro* and imaged by confocal microscopy to quantitate *uv*-bPNMP and Cy5-pLUC fluorescence remaining on the microneedle surfaces. After 15 min incubation in PBS, we observed a significant loss of both bPNMP and Cy5-pLUC fluorescence from microneedle arrays (Supplementary Fig. S3). By contrast, no film release was observed if PEMs were assembled onto PNMP coatings that had not been irradiated to photo-switch the release-layer's solubility. To determine whether microneedles coated with releasable films would permit rapid multilayer implantation *in vivo*, we applied dry (PNMP/PEM)-coated microneedles to the auricular skin of C57Bl/6-MHC II-GFP mice[26]. Trypan blue staining of treated skin in this case showed consistent microneedle insertion (Fig. 3a). Mirroring our *in vitro* observations, confocal imaging of microneedles after 15 min application to murine skin showed that both *uv*-bPNMP and Cy5-pLUC fluorescence was rapidly lost from coated microneedles, but only if PNMP films were irradiated before multilayer assembly to prime for rapid dissolution of the release-layer (Fig. 3b,c). Confocal imaging of skin samples following application of (PNMP/PEM)-coated microneedles for 15 min showed significant transfer of Cy5-pLUC in the epidermis co-localized with MHC II-GFP$^+$ Langerhans cells (LCs; Fig. 3d) and up to 400 μm deep into the skin (Fig. 3e), but only when the PNMP layer was ultraviolet-primed. Similarly, microneedles carrying poly(I:C)-loaded PEM films deposited fluorescently labelled poly(I:C) into the skin, colocalizing in the same *z*-plane with MHC II-GFP-expressing cell populations (Fig. 3f). Twenty-four hours after implantation of (poly-1/nucleic acid) multilayers, the

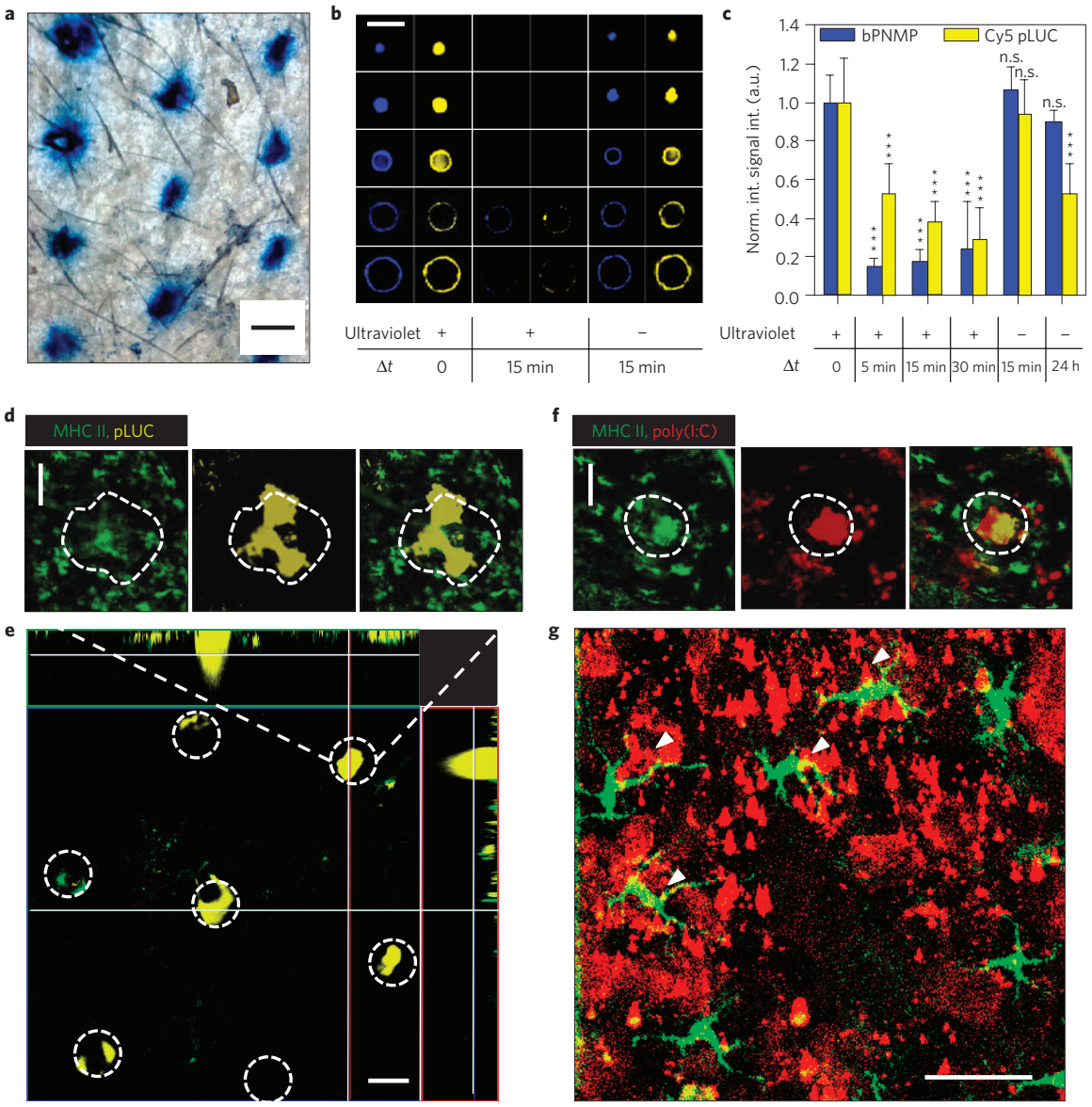

Figure 3 | PNMP release-layers promote rapid implantation of multilayer films at microneedle penetration sites *in vivo*. **a**, Optical micrograph of ear skin stained with trypan blue to reveal epidermal penetration following PLLA microneedle application (scale bar, 500 μm). **b**, Representative confocal images of (SAv488-bPNMP)(PS/SPS)$_{20}$(poly-1/Cy5-pLUC)$_{35}$-coated PLLA microneedles with or without ultraviolet sensitization of the PNMP layer (blue, Sav488-bPNMP; yellow, Cy5-pLUC), before application, or after 15 min application to murine ear skin (lateral sections, 100 μm *z*-intervals, scale bar, 200 μm). **c**, Quantitation of confocal fluorescence intensities ($n = 15$) showing loss of Sav488-*uv*-bPNMP and Cy5-pLUC films from coated microneedles on application to skin, dependent on ultraviolet-induced photo-switching of the PNMP layer solubility. Data represent the mean ± s.e.m., $***, p < 0.0001$, analysed by the unpaired *t*-test. **d**, Representative confocal image of treated murine skin showing film implantation after 15 min (green, MHC II-GFP; yellow, Cy5-pLUC; penetration site outlined; scale bar, 100 μm). **e**, *x-y/x-z/y-z* confocal images showing depth of Cy5-pLUC film deposition after 15 min microneedle application (green, MHC II-GFP; yellow, Cy5-pLUC; penetration sites outlined; scale bar, 200 μm). **f**, Representative confocal image of treated murine skin showing TMR-poly(I:C) film implantation after 15 min microneedle application (green, MHC II-GFP; red, TMR-poly(I:C); penetration site outlined; scale bar, 100 μm). **g**, Colocalization and uptake of TMR-poly(I:C) by MHC II-GFP$^+$ LCs at the microneedle insertion site 24 h following film implantation (green, MHC II-GFP; red, TMR-poly(I:C); yellow, overlay; scale bar, 50 μm).

degrading films were observed dispersed into the tissue around the needle insertion site and showed apparent uptake in colocalized LCs (Fig. 3g). Thus, the *uv*-PNMP release-layer promotes rapid transfer of DNA- or RNA-loaded films from microneedles into the skin.

We next tested whether the *in vivo* kinetics of nucleic acid release into the surrounding tissue could be controlled via the composition of multilayers implanted in the skin. Past studies have demonstrated the ability of multilayers composed of pDNA assembled with the PBAEs poly-1 or poly-2 to mediate release with varying kinetics[27,28]. Consistent with this previous work, (PS/SPS)$_{20}$(poly-1/poly(I:C))$_{35}$ and (PS/SPS)$_{20}$(poly-1/pLUC)$_{35}$ multilayers constructed on Si substrates exhibited rapid release at 37 °C of ~80% pLUC or poly(I:C) within 24 h, whereas analogous films constructed with poly-2 showed a slower release lasting ~1 week (Supplementary Fig. S4). To determine whether the composition of PBAE multilayers implanted via microneedle delivery could mediate similar tunable release of nucleic acid therapeutics *in vivo*, we constructed (PBAE/Cy5-poly(I:C)) PEM films on

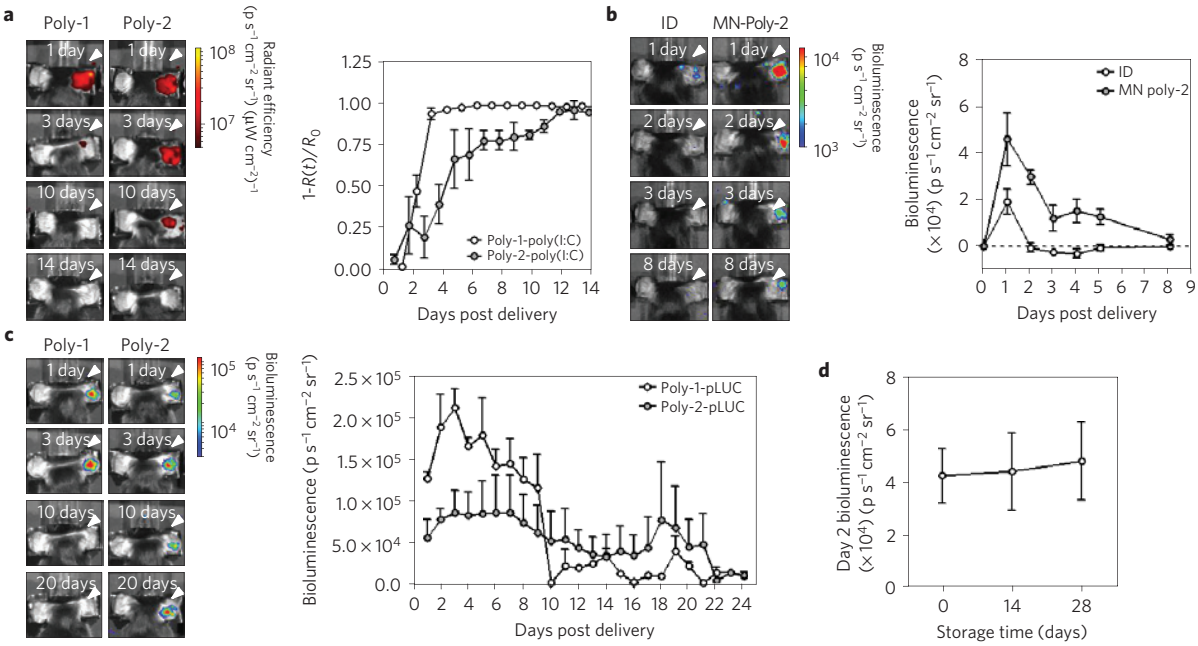

Figure 4 | Implanted films control the physical and functional persistence of pDNA and poly(I:C) *in vivo*. **a**, Representative whole-animal fluorescence images showing TMR-poly(I:C) retention at the application site and quantitative analysis of normalized total fluorescence $R(t)$ relative to initial fluorescence R_o from groups of animals ($n = 3$) over time following 15 min application of PLLA microneedles coated with (*uv*-PNMP)(PS/SPS)$_{20}$(PBAE/TMR-poly(I:C))$_{35}$ multilayers containing poly-1 or poly-2 as the PBAE component. Data represent the mean ± s.e.m. **b**, Representative whole-animal luminescent images and quantitative analysis of luminol signal from MPO-dependent oxidative burst in activated phagocytes at the treatment site over time following intradermal injection of 10 μg poly(I:C) or 15 min application of PLLA microneedles coated with (*uv*-PNMP)(PS/SPS)$_{20}$(poly-2/poly(I:C))$_{35}$ multilayers. Data represent the mean ± s.e.m., $n = 4$. **c**, Representative whole-animal bioluminescence images of pLUC expression at the application site and mean bioluminescence intensity over time following 15 min application of microneedles coated with (*uv*-PNMP)(PS/SPS)$_{20}$(PBAE/pLUC)$_{35}$ multilayers containing poly-1 or poly-2 as the PBAE component. Data represent the mean ± s.e.m., $n = 4$. **d**, Mean bioluminescent intensity on day 2 following 15 min application of microneedles coated with (*uv*-PNMP)(PS/SPS)$_{20}$(Poly-1/pLUC)$_{35}$ multilayers stored dry at 25 °C for 0, 14 or 28 days. Data represent the mean ± s.e.m., $n = 4$.

uv-PNMP-coated microneedles using poly-1 or poly-2 as the PBAE component. Following application of coated microneedles to the skin of C57Bl/6 mice for 15 min, we monitored the fluorescence signal of implanted Cy5-poly(I:C) over time using whole-animal fluorescence imaging. Similar to the *in vitro* trend, films encapsulating poly(I:C) with poly-1 were quickly cleared from the application site, whereas (poly-2/poly(I:C)) films persisted for ten days following application (Fig. 4a). To quantify the functional impact of sustained polyI:C adjuvant release *in vivo*, we applied microneedles carrying (poly-2/poly(I:C)) multilayers to the auricular skin of mice or injected equivalent doses of free poly(I:C) intradermally at the same site, and administered the chemiluminescent probe luminol to trace local inflammation over time. Systemically injected luminol emits photons when catabolized by myeloperoxidase (MPO) produced by activated innate immune cells at sites of inflammation[29,30]. As shown in Fig. 4b, bolus poly(I:C) injection elicited a transient burst of inflammation that resolved by 48 h, whereas multilayer implantation resulted in 2-fold higher peak MPO activity at 24 h that decayed slowly to baseline over ~1 week. Importantly, poly(I:C)-triggered inflammation was highly localized to the application site, as no elevation of systemic cytokines was observed following multilayer implantation (data not shown). Thus, the composition of implanted PEM films can directly control the kinetics of release and local inflammatory response in the skin.

The selection of poly-1 and poly-2 as biodegradable polycation components of these PEM coatings was motivated not only by their ability to regulate nucleic acid release, but also to directly promote transfection by forming pDNA polyplexes *in situ* during film degradation[21,31]. Dynamic light scattering analysis of supernatants collected from these eroded films *in vitro* revealed large aggregates (50–300 nm, data not shown), consistent with previous evidence of *in situ* polyplex formation/release from degrading (PBAE/pDNA) multilayers[27,31]. To determine whether controlled polyplex release from implanted films would allow gene expression kinetics to be regulated *in vivo*, we used bioluminescence imaging to monitor expression of luciferase-encoding DNA longitudinally in live animals. Although *in vivo* optical imaging analysis of bioluminescent signals is limited by variable photon penetration from different tissue depths and locations, it is useful for accurate comparison of relative signals from identical tissue sites and for longitudinal analysis of the duration of expression. Microneedles were prepared with (PNMP/PEM) coatings containing pLUC as before, with or without ultraviolet-priming of the PNMP release-layer. We verified that pDNA released from multilayers *in vitro* retained bioactivity over the entire course of film degradation comparable to fresh PBAE/DNA polyplexes (Supplementary Fig. S5). *In vivo*, control microneedles (where the release-layer was not ultraviolet-primed) applied to the skin of mice for 15 min led to no detectable expression of pLUC by bioluminescence imaging (Supplementary Fig. S6), consistent with the lack of detectable film transfer into skin under this condition. By contrast, mice treated with microneedles coated with (*uv*-PNMP/PEM) films showed significant levels of bioluminescence one day after application, demonstrating transfection of cells *in situ* (Fig. 4c). Further, the kinetics of pLUC expression varied greatly depending on the PBAE used: delivery of (poly-1/pLUC) multilayers led to luciferase expression that peaked after three days and declined to background levels after

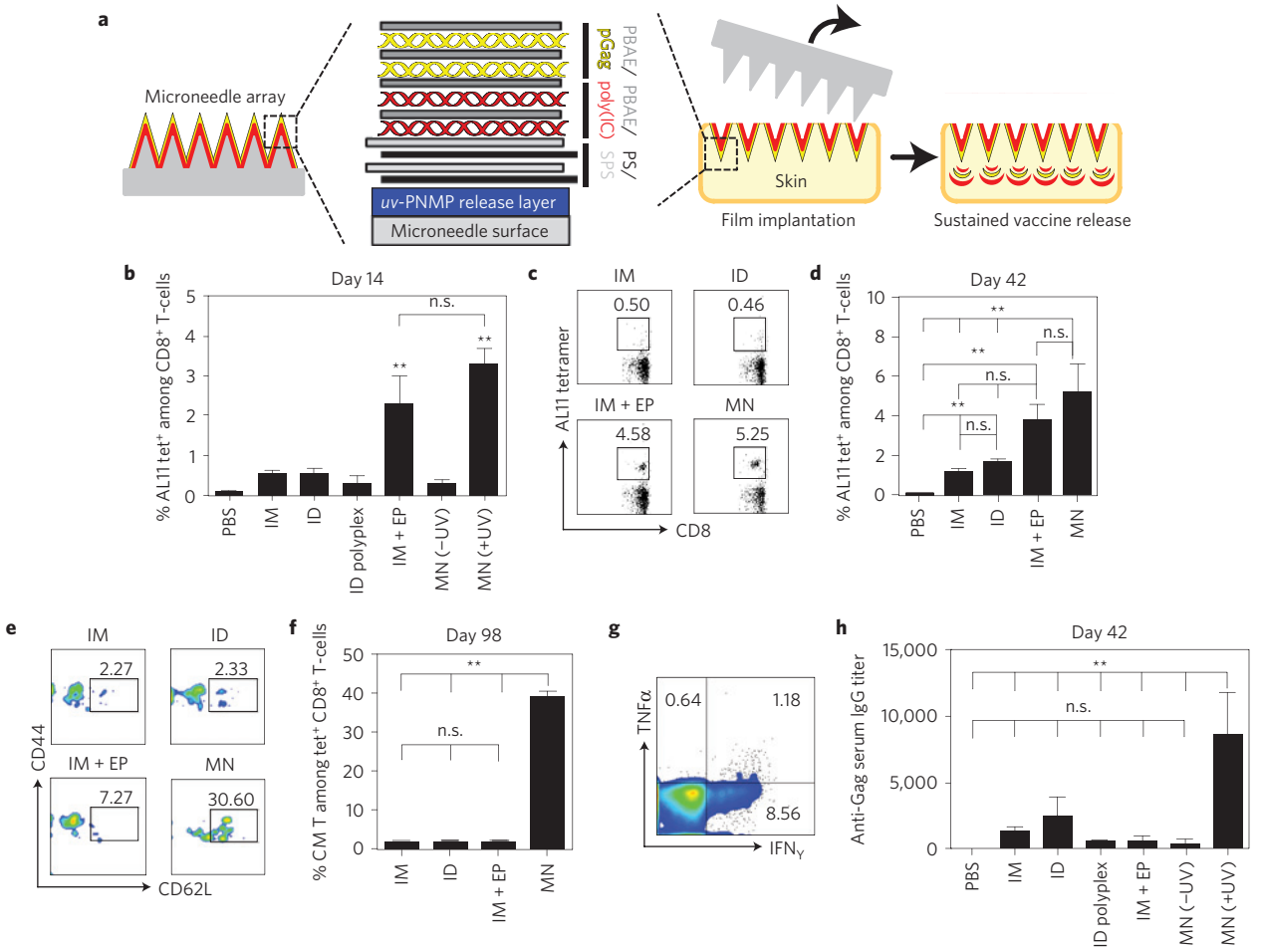

Figure 5 | Microneedle tattooing with multilayer films carrying pDNA and poly(I:C) generates potent cellular and humoral immunity against a model HIV antigen. a, C57Bl/6 mice ($n = 4$ mice per group) were immunized with 20 μg pGag and 10 μg poly(I:C) on days 0 and 28 intramuscularly (with or without electroporation (EP)) in the quadriceps, intradermally in the dorsal ear skin (with free pGag or pGag/poly-1 polyplexes, ID ± Polyplex), or by 15 min application of (PNMP)$(PS/SPS)_{20}$(poly-1/poly(I:C))$_{35}$(poly-1/pLUC)$_{35}$-coated microneedles with or without ultraviolet-priming of the PNMP release-layer (MN ± UV) to the dorsal ear skin. **b**–**d**, Frequency of Gag-specific $CD8^+$ T-cells in peripheral blood assessed by flow cytometry analysis of tetramer$^+$$CD8^+$ T-cells. Shown are mean ± s.e.m. tetramer$^+$ values from day 14 (**b**), representative cytometry plots from individual mice (**c**), and mean ± s.e.m. tetramer$^+$ values from day 42 (**d**). **e**,**f**, Analysis of T-cell effector/central memory phenotypes in peripheral blood by CD44/CD62L expression of tetramer$^+$ cells from peripheral blood. Shown are representative cytometry plots from individual mice at day 49 (**e**) and mean ± s.e.m. percentages of tetramer$^+$$CD44^+$$CD62L^+$ among $CD8^+$ T-cells at day 98 (**f**). **g**, Mice immunized with microneedles were recalled on day 105 by IM injection of 50 μg pGag, and assessed for cytokine production on *ex vivo* restimulation with AL11 peptide on day 112. Shown is representative flow cytometry analysis of IFN-γ/TNFα-producing $CD8^+$ T-cells. **h**, Enzyme-linked immunosorbent assay analysis of total Gag-specific IgG in sera at day 42. Data represent the mean ± s.e.m., $**P < 0.005$, analysed by two-way ANOVA.

ten days, whereas implantation of slower-degrading (poly-2/pLUC) films showed prolonged bioluminescence, peaking on day 3 then slowly decreasing to background levels by day 22 (Fig. 4c). Together this data shows that multilayer tattooing can be used to tailor the duration of both inflammatory signals and antigen-encoding DNA expression *in vivo*, via selection of constituent polymers with varying degradation rates.

Embedding bioactive molecules in multilayer films has previously been shown to enhance their stability for dry-state storage at room temperature[16,17], an attractive feature for vaccines given the costs and availability limitations imposed by the need for refrigeration of liquid vaccine formulations. To test whether (PBAE/pDNA) multilayer films coated on microneedles stabilize their DNA cargo for dry storage, we fabricated microneedle arrays coated with (*uv*-PNMP/PEM) films and stored them dry at 25 °C for 0, 14 or 28 days before application to the skin of mice as before. Bioluminescence imaging of these animals after treatment revealed no significant decrease in transfection resulting from storage, indicating the maintenance of pDNA bioactivity in multilayers for extended durations (Fig. 4d). These results suggest that microneedles coated with vaccine-containing multilayers could be easily packaged for inexpensive dry-state storage and transportation to remote areas of the world, bypassing the 'cold-chain' requirements of conventional vaccines.

Previous work has demonstrated DNA uptake in both keratinocytes and local APCs following delivery to the skin in both humans and mice, both of which can contribute to induction of immune responses in DNA vaccination (reviewed in ref. 32). To test the ability of multilayer tattooing with vaccine-loaded polymer films to enhance DNA immunization, we coated microneedles with (*uv*-PNMP)$(PS/SPS)_{20}$(poly-1/poly(I:C))$_{35}$(poly-1/pGag)$_{35}$ composite releasable multilayers containing the adjuvant poly(I:C) and pGag, a plasmid encoding the model HIV antigen SIV-*gag* (Fig. 5a). We compared multilayer tattooing to several

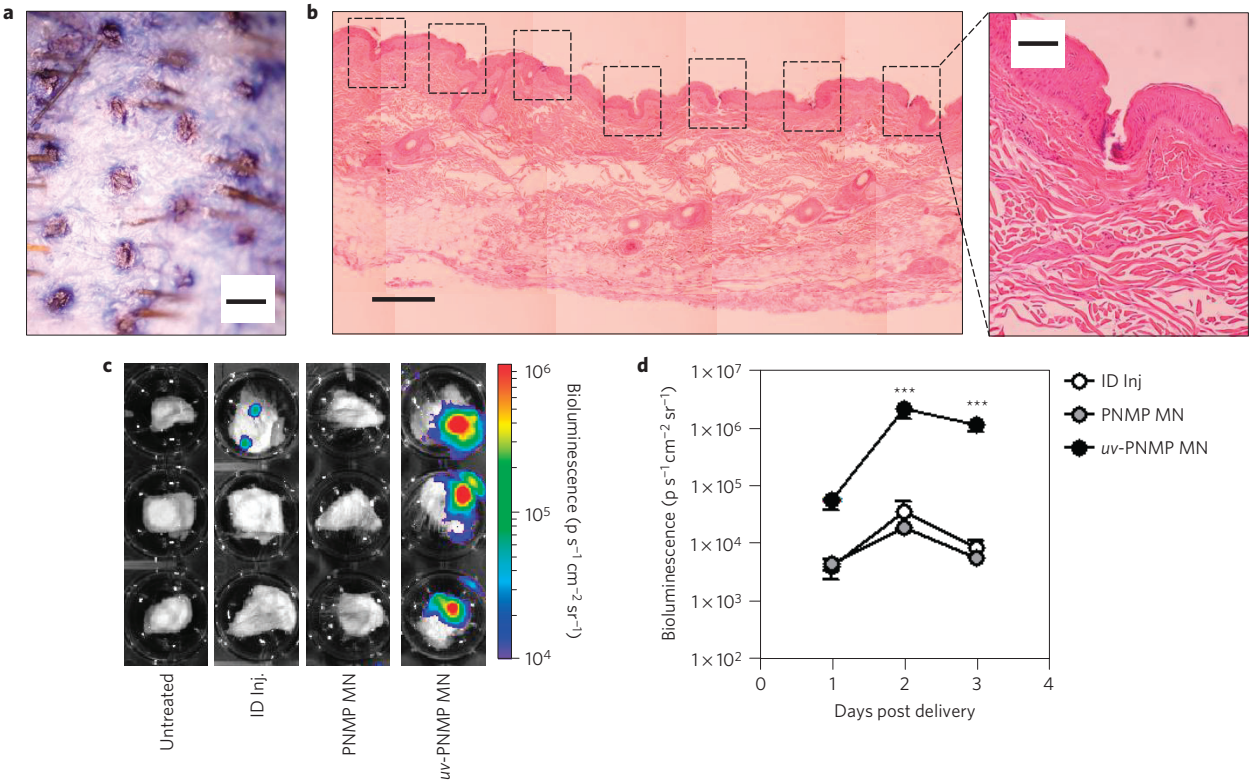

Figure 6 | Multilayer tattooing enhances transfection in non-human primate skin. a, Optical micrograph of macaque quadriceps skin showing microneedle penetration pattern stained using trypan blue (scale bar, 500 μm). **b**, Histological section of microneedle-treated macaque skin showing epidermal disruption at microneedle insertion sites (boxed, left, scale bar, 500 μm; right, scale bar, 100 μm). **c**, Bioluminescence images of luciferase expression 2 days after pLUC delivery by ID injection or microneedle tattooing with $(PS/SPS)_{20}(poly\text{-}1/pLUC)_{35}$ films from either *uv*-PNMP- or non-irradiated PNMP-coated microneedles following a 15 min application. **d**, Quantification of total bioluminescent signal in cultured skin tissue explants 1, 2 and 3 days after treatment. Data represent the mean ± s.e.m., $n = 3$. ***, $p < 0.0001$, analysed by an unpaired *t*-test.

control immunizations using the same delivered dose of pGag and poly(I:C): injection of 'naked' pDNA, the most common experimental strategy for DNA immunization in mice and humans; and *in vivo* electroporation, where DNA is administered in the presence of an electric field to promote DNA uptake[4,33]. To confirm the importance of the pH-responsive release-layer, we also tested microneedles where the PNMP layer was not ultraviolet-treated, and hence unable to dissolve on skin insertion. Finally, we also compared immune responses in mice receiving intradermal injections of poly-1/pGag polyplexes, to determine the importance of the sustained-release multilayer film architecture for generating immunity. In all cases we immunized groups of animals on days 0 and 28 with 20 μg pGag and 10 μg poly(I:C). Multilayer tattooing was performed with microneedles (MN ± UV) applied to the dorsal ear skin for 15 min. Control mice were injected intradermally (ID and ID Polyplex) in the ear skin, or intramuscularly with or without *in vivo* electroporation (IM ± EP). Peptide-MHC tetramer staining of peripheral blood mononuclear cells showed that IM and ID ± Polyplex administration produced only weak antigen-specific $CD8^+$ T cell responses (Fig. 5b–d). By contrast, microneedle-treated groups showed robust expansion of Gag-reactive T-cells, exceeding 5% of the circulating $CD8^+$ population two weeks after the boost, a response that was quantitatively similar to frequencies observed for IM + EP immunized mice (Fig. 5b–d). Notably, the response to MN vaccination was ablated if the PNMP release-layer was not ultraviolet-treated (and was therefore unable to dissolve on application). Moreover, compared to all of the other vaccination regimens, microneedle administration generated substantially greater frequencies of $CD44^+CD62L^+$ central memory T-cells, a population thought to be important for recall immunity and long-term protection (Fig. 5e,f)[34]. Following injection of naked pDNA 3.5 months after the prime to test recall responses, large frequencies of IFN-γ-producing $CD8^+$ T-cells were elicited (Fig. 5g), suggesting the establishment of robust T-cell memory. Finally, two weeks after the boost, we measured total Gag-specific IgG titers in sera and observed a 10-fold increase in microneedle-treated mice over those given any other immunization regimen ($P < 0.01$; Fig. 5h). Thus, DNA vaccination via multilayer tattooing shows the potential to match (or exceed) the potency of *in vivo* electroporation, using a skin patch that can be stored in a dry state, is painlessly applied with no extraneous apparatus, and could be self-applied in minutes.

Although naked DNA injections stimulate immune responses in small animals, responses observed in non-human primates and humans have been much weaker[1–3]. To determine whether multilayer tattooing could also enhance the efficacy of DNA delivery in non-human primates, we tested the ability of PNMP-coated microneedles to deliver (poly-1/pLUC) multilayers into fresh explanted skin from Rhesus macaques *ex vivo*. Trypan blue staining and histological sectioning of macaque skin treated with uncoated PLLA microneedles showed uniform patterns of microneedle insertion into the superficial layers of the skin without disruption of underlying dermal layers or capillary vessels (Fig. 6a,b). We tested the ability of microneedles coated with (*uv*-PNMP/PEM) films to transfect *ex vivo* cultured macaque skin explants compared to intradermal injections of equivalent doses of naked pDNA. Microneedles coated with (PNMP/PEM) multilayers effectively transfected macaque skin explants following a 15 min application period, but, as in mice, transfection only occurred

if the PNMP release-layer was ultraviolet-primed for dissolution (Fig. 6c). Bioluminescence imaging of the treated skin samples showed that microneedle delivery generated consistent expression of luciferase at 140-fold greater levels compared to intradermally injected naked DNA controls for several days ($P < 0.01$, Fig. 6d). Previous results in mice have indicated that the magnitude of gene expression following DNA vaccination correlates with the strength of T-cell responses *in vivo*[35]. Thus, although the limitations of *ex vivo* skin explant culture prevent measurement of the long-term duration of gene expression, these results indicate that microneedle delivery promotes strong initial DNA expression in non-human primate skin, where naked DNA injection elicits very weak transfection only a few fold above background. Although the magnitude of gene expression is only one parameter determining the ultimate strength of immune responses following DNA vaccination, the ability to improve expression levels in primates is a significant result, given that poor transfection efficiency is an acknowledged obstacle for improving DNA immunogenicity in large animal models and humans[33,36].

Microneedles have recently shown substantial promise in vaccine delivery[37,38], and several reports have begun to explore the use of metal microneedles to deliver DNA into the skin[39–42]. These studies have demonstrated the ability of naked DNA delivery by microneedles to provide enhanced immune responses compared to intramuscular injection, but only one study compared microneedle administration to alternative approaches designed to elicit improved transfection; in that test microneedles elicited T-cell responses comparable to gene gun delivery of DNA if twice the DNA dose was given by the microneedle array[40]. Here we have demonstrated a new approach for DNA vaccination via multilayer 'tattooing', using microneedles employing a pH-responsive release-layer to rapidly implant biodegradable vaccine-loaded polymer films into the skin. (Note that this new approach should not be confused with earlier studies of 'DNA tattooing', where DNA solutions are literally applied to the skin using a commercial tattoo device[9,33,43]—a completely different method.) Multilayer tattooing simultaneously addresses several issues in DNA vaccine delivery: implanted multilayers deliver DNA with transfection agents, promoting transfection *in situ*; molecular adjuvants are co-delivered to amplify the immune response; and we have shown that the multilayer structure allows the kinetics of vaccine release to be tailored over days to weeks. Combined, these features enabled multilayer tattooing to elicit immune responses in mice far exceeding naked DNA injections. These responses were also comparable to *in vivo* electroporation, an approach currently viewed as a gold standard for experimental DNA vaccine potency but which requires special equipment, elicits pain and discomfort in recipients[44,45], and is unlikely to be feasible in widespread prophylactic vaccination. Notably, vaccines have been shown to vary widely in potency based on the duration of exposure to antigen and adjuvant combinations[9–12]. Our studies suggest that the continuous release of polyplexes from implanted multilayers may be critical to the enhanced immunogenicity of multilayer tattooing, as bolus injection of free polyplexes formed from the same components elicited very weak immune responses. Finally, we have shown that formulation of DNA vaccines as multilayer coatings on microneedles provides the opportunity for long-term maintenance of DNA bioactivity in a dried state without refrigeration, addressing cost and availability limitations imposed by the cold-chain in the global distribution and storage of vaccines. We focused here on DNA vaccination owing to the relevance of needle-free vaccines for global health and the need for enhanced DNA vaccination strategies. However, the well-known adaptability of multilayers for incorporation and controlled release of diverse therapeutics[15,46–51] suggests this approach should be applicable to diverse drug delivery applications. Further, the pH-sensitive release-layer strategy employed here is a generalizable approach to create selectively released multilayer films. Although the true potential of any vaccination strategy can only be established in human clinical trials, the data shown here suggest that multilayer tattooing is a promising approach to enhance the efficacy of DNA vaccines, a platform technology with the potential to be applied universally in vaccine development.

Methods

Materials. bPNMP (31:59:10 oNBMA:MMA:PEGMA by mol, 17 kDa), poly-1 (15 kDa), and poly-2 (20 kDa) were synthesized as previously reported[18,24]. AL-11/H-2K^b-peptide-MHC II tetramers were provided by the NIH tetramer core facility.

PLLA microneedle fabrication. PDMS moulds (Sylgard 184, Dow-Corning) were prepared using a Clark-MXR-CPA-2010 (VaxDesign). PLLA (IV 1.9 dl g^{-1}, Lakeshore Biomaterials) was melted over the moulds under vacuum (−25 in. Hg, 200 °C, 40 min), and then cooled to −20 °C before removal and crystallization at 140 °C for 4 h for solvent resistance.

PNMP release-layer deposition. On Si substrates, 3 wt% PNMP in 1,4-dioxane was deposited using a Specialty Coating Systems P6700 (Indianapolis). On PLLA microneedles, 0.25 wt% bPNMP was spray deposited as previously described (0.2 ml s^{-1}, 15 cm range, 10 s; ref. 20). Films were dried under vacuum at 25 °C for 12 h. bPNMP release-layers were labelled with Alexafluor-488-conjugated-SAv (10 μg ml^{-1} in PBS pH 6.0, Sigma-Aldrich).

Polymer multilayer film preparation. LbL films were assembled using a Carl Ziess HMS-DS50 stainer. Films were constructed on Si wafers and PLLA microneedles following deposition of bPNMP and photoswitching via ultraviolet irradiation (254 nm, 2.25 mW cm^{-2}) for 15 min. (PS/SPS) base layers were deposited through alternative immersion into PS (2 mg ml^{-1}, Sigma-Aldrich) and SPS (5 mM, Sigma-Aldrich) for 10 min, separated by two 1 min PBS rinses. (PBAE/nucleic acid) multilayers were deposited similarly, alternating 5 min dips in poly-1/2 (2 mg ml^{-1}) and either pLUC, pGag, or poly(I:C) (Invivogen) solutions (1 mg ml^{-1}) separated by two 30 s PBS rinses. Fluorescent pLUC and poly(I:C) were prepared using Cy5 and tetramethyl-rhodamine (TMR) Label-IT reagent (Mirus Bio). All solutions were in PBS, adjusted to pH 5.0. Films were characterized using a Veeco Dektak profilometer and a Zeiss LSM510. Normalized integrated signal intensities (Norm. int. signal int.) were determined by integrating the total confocal fluorescence signal from *z*-stacks collected through the length of individual microneedles following various treatments and normalizing to the total initial fluorescence on the as-fabricated microneedles. Data analysis was performed using Image J. Film loading was determined using a SpectraMax 250 following elution of films in PBS, pH 7.4, 2M NaCl for 24 h.

***In vitro/in vivo* delivery.** For *in vitro* release experiments, $(PS/SPS)_{20}(PBAE/nucleic\ acid)_{35}$ films were incubated in PBS at 37 °C and aliquots were assayed for pLUC or poly(I:C) using picogreen or ribogreen assay kits (Invitrogen). For *in vitro* delivery, coated microneedles were incubated in PBS, pH 7.4 and imaged by confocal microscopy. *In vivo* delivery experiments were performed on anesthetized C57BL/6 mice (Jackson Laboratories) and MHC II-GFP transgenic mice (a gift from H. Ploegh)[26]. Ears were rinsed with PBS on the dorsal side and dried before application of microneedle arrays by gentle pressure. Applied microneedles were imaged by confocal microscopy. Treated skin was excised and stained with trypan blue for needle penetration. Ears treated with Cy5-pLUC- or TMR-poly(I:C)-coated microneedles (with or without ultraviolet treatment) were mounted and imaged by confocal microscopy. Clearance of fluorescent poly(I:C) and transfection in mice treated with pLUC-coated arrays (with or without ultraviolet treatment) was measured using an IVIS Spectrum 200 (Caliper Lifesciences). For luminescent measurements of pLUC expression, mice were imaged following IP administration of D-luciferin (150 mg kg^{-1}). For luminescent imaging of MPO-dependent oxidative burst, luminol sodium salt (Santa Cruz Biotech) was administered IP (250 mg kg^{-1}) before imaging as previously described[29]. Fluorescence/bioluminescence data was processed using region of interest (ROI) analysis with background subtraction and internal control ROI comparison to untreated skin using the Living Image 4.0 software package (Caliper).

Vaccinations. Animal studies were approved by the MIT IUCAC and animals were cared for in the USDA-inspected MIT Animal Facility under federal, state, local, and NIH guidelines for animal care. Groups of 4 C57Bl/6 mice were immunized with 20 μg pGag and 10 μg poly(I:C) by intramuscular injection (15 μl, quadriceps) with or without *in vivo* electroporation (Harvard Apparatus ECM830, 2 × 60 ms pulses, 200 V cm^{-1}), intradermal injection (15 μl, dorsal ear skin, poly(I:C) mixed with free DNA or DNA/poly-1 polyplexes), or by microneedle array (15 min application of $(PS/SPS)_{20}(poly\text{-}1/poly(I:C))_{35}(poly\text{-}1/pGag)_{35}$ on *uv*-PNMP and native-PNMP coated PLLA arrays). To form poly-1/pDNA polyplexes, pDNA was

mixed as previously described with PBAE (1:1 ratio by mass) in deionized water and vortexed briefly before injection[52]. All animals received the same delivered doses of pGag and poly(I:C); microneedle-delivered dosages were determined by comparison of total eluted pDNA from coated arrays before and after treatment. Frequencies of Gag-specific $CD8^+$ T-cells and their phenotypes were determined by flow cytometry analysis of peripheral blood mononuclear cells following staining with DAPI (live/dead), anti-CD8α, anti-CD44, anti-CD62L, and AL-11/H-2 K^b-peptide-MHC tetramers. Anti-Gag IgG titers, defined as the dilution of sera at which the OD reading was 0.25, were determined by ELISA using SIV-mac251 (My Biosource) coated plates, and ultraviolet–visible detection of peroxidase conversion of tetramethybenzydine (KPL) using HRP-conjugated anti-IgG (Jackson Immunoresearch). To assess recall responses, microneedle-treated animals were challenged with 50 μg intramuscular pGag in the quadriceps and cytokine expression was measured by flow cytometry in peripheral blood mononuclear cells following stimulation with AL11 peptide, treatment with brefeldin A, and staining with DAPI, anti-CD8α, and anti-IFNγ, anti-TNFα.

***Ex vivo* macaque skin culture and microneedle testing.** Macaque studies were approved by the Harvard Medical School IACUC. Outbred Rhesus monkeys were housed at New England Primate Research Center. Fresh skin was obtained from the quadriceps of euthanized Rhesus macaques. Skin was mounted on slides and microneedles were applied by gentle pressure. Skin was stained using trypan blue for needle insertion, formaldehyde fixed, and embedded in paraffin for histological sectioning, hemotoxylin and eosin staining, and optical imaging. To assay *ex vivo* transfection, pLUC was injected intradermally (20 μg in 10 μl PBS) or delivered by microneedle in $(PS/SPS)_{20}(poly\text{-}1/pLUC)_{35}$ multilayers overlying native or *uv*-PNMP. Skin was cultured as previously described[53] and imaged using an IVIS Spectrum after addition of 300 μg luciferin to the culture media. Data analysis was performed as before, using the Living Image Software package.

Statistical analysis. Statistical analysis was performed with Graphpad Prism using two-way analysis of variance or *t*-test. Values are reported as mean ± s.e.m.

Received 18 June 2012; accepted 13 December 2012; published online 27 January 2013

References

1. Kutzler, M. A. & Weiner, D. B. DNA vaccines: Ready for prime time? *Nature Rev. Genet.* **9,** 776–788 (2008).
2. Rice, J., Ottensmeier, C. H. & Stevenson, F. K. DNA vaccines: Precision tools for activating effective immunity against cancer. *Nature Rev. Cancer* **8,** 108–120 (2008).
3. Ulmer, J. B., Wahren, B. & Liu, M. A. Gene-based vaccines: Recent technical and clinical advances. *Trends Mol. Med.* **12,** 216–222 (2006).
4. Sardesai, N. Y. & Weiner, D. B. Electroporation delivery of DNA vaccines: Prospects for success. *Curr. Opin. Immunol.* **23,** 421–429 (2011).
5. Weir, E. & Hatch, K. Preventing cold chain failure: Vaccine storage and handling. *Can. Med. Assoc. J.* **171,** 1050 (2004).
6. Rapiti, E., Pruss-Ustun, A. & Hutin, Y. *WHO Environmental Burden of Disease Series* (World Health Organization, 2003).
7. Dicko, M. *et al.* Safety of immunization injections in Africa: Not simply a problem of logistics. *Bull. World Health Org.* **78,** 163–169 (2000).
8. Giudice, E. L. & Campbell, J. D. Needle-free vaccine delivery. *Adv. Drug Deliv. Rev.* **58,** 68–89 (2006).
9. Bins, A. D. *et al.* A rapid and potent DNA vaccination strategy defined by *in vivo* monitoring of antigen expression. *Nature Med.* **11,** 899–904 (2005).
10. Johansen, P. *et al.* Antigen kinetics determines immune reactivity. *Proc. Natl Acad. Sci. USA* **105,** 5189–5194 (2008).
11. Jewell, C. M., Bustamante, L. S. C. & Irvine, D. J. *In situ* engineering of the lymph node microenvironment via intranodal injection of adjuvant-releasing polymer particles. *Proc. Natl Acad. Sci. USA* **108,** 15745–15750 (2011).
12. Prlic, M., Hernandez-Hoyos, G. & Bevan, M. J. Duration of the initial TCR stimulus controls the magnitude but not functionality of the CD8+ T cell response. *J. Exp. Med.* **203,** 2135–2143 (2006).
13. Decher, G. Fuzzy nanoassemblies: Toward layered polymeric multicomposites. *Science* **277,** 1232–1237 (1997).
14. Hammond, P. T. Engineering materials layer-by-layer: Challenges and opportunities in multilayer assembly. *AIChE J.* **57,** 2928–2940 (2011).
15. Macdonald, M., Rodriguez, N. M., Smith, R. & Hammond, P. T. Release of a model protein from biodegradable self assembled films for surface delivery applications. *J. Controlled Release* **131,** 228–234 (2008).
16. MacDonald, M. L. *et al.* Tissue integration of growth factor-eluting layer-by-layer polyelectrolyte multilayer coated implants. *Biomaterials* **32,** 1446–1453 (2011).
17. Shah, N. J. *et al.* Tunable dual growth factor delivery from polyelectrolyte multilayer films. *Biomaterials* **32,** 6183–6193 (2011).
18. Doh, J. & Irvine, D. J. Photogenerated polyelectrolyte bilayers from an aqueous-processible photoresist for multicomponent protein patterning. *J. Am. Chem. Soc.* **126,** 9170–9171 (2004).
19. DeMuth, P. C., Su, X., Samuel, R. E., Hammond, P. T. & Irvine, D. J. Nano-layered microneedles for transcutaneous delivery of polymer nanoparticles and plasmid DNA. *Adv. Mater.* **22,** 4851–4856 (2010).
20. Krogman, K. C., Lowery, J. L., Zacharia, N. S., Rutledge, G. C. & Hammond, P. T. Spraying asymmetry into functional membranes layer-by-layer. *Nature Mater.* **8,** 512–518 (2009).
21. Jewell, C. M., Zhang, J., Fredin, N. J. & Lynn, D. M. Multilayered polyelectrolyte films promote the direct and localized delivery of DNA to cells. *J. Controlled Release* **106,** 214–223 (2005).
22. Katz, J. S., Doh, J. & Irvine, D. J. Composition-tunable properties of amphiphilic comb copolymers containing protected methacrylic acid groups for multicomponent protein patterning. *Langmuir* **22,** 353–359 (2006).
23. Little, S. R. *et al.* Poly-β amino ester-containing microparticles enhance the activity of nonviral genetic vaccines. *Proc. Natl Acad. Sci. USA* **101,** 9534–9539 (2004).
24. Lynn, D. M. & Langer, R. Degradable poly(β-amino esters): Synthesis, characterization, and self-assembly with plasmid DNA. *J. Am. Chem. Soc.* **122,** 10761–10768 (2000).
25. Su, X., Kim, B-S., Kim Sara, R., Hammond Paula, T. & Irvine Darrell, J. Layer-by-layer-assembled multilayer films for transcutaneous drug and vaccine delivery. *ACS Nano* **3,** 3719–3729 (2009).
26. Boes, M. *et al.* T-cell engagement of dendritic cells rapidly rearranges MHC class II transport. *Nature* **418,** 983–988 (2002).
27. Jewell, C. M. *et al.* Release of plasmid DNA from intravascular stents coated with ultrathin multilayered polyelectrolyte films. *Biomacromolecules* **7,** 2483–2491 (2006).
28. Zhang, J., Fredin, N. J., Janz, J. F., Sun, B. & Lynn, D. M. Structure/property relationships in erodible multilayered films: Influence of polycation structure on erosion profiles and the release of anionic polyelectrolytes. *Langmuir* **22,** 239–245 (2006).
29. Gross, S. *et al.* Bioluminescence imaging of myeloperoxidase activity *in vivo*. *Nature Med.* **15,** 455–461 (2009).
30. Soria-Castro, I. *et al.* Cot/tpl2 (MAP3K8) mediates myeloperoxidase activity and hypernociception following peripheral inflammation. *J. Biol. Chem.* **285,** 33805–33815 (2010).
31. Bechler, S. L. & Lynn, D. M. Characterization of degradable polyelectrolyte multilayers fabricated using DNA and a fluorescently-labeled poly(β-amino ester): Shedding light on the role of the cationic polymer in promoting surface-mediated gene delivery. *Biomacromolecules* **13,** 542–552 (2012).
32. Elnekave, M., Furmanov, K. & Hovav, A-H. Intradermal naked plasmid DNA immunization: Mechanisms of action. *Expert Rev. Vaccines* **10,** 1169–1182 (2011).
33. Van Drunen Littel-van den Hurk, S. & Hannaman, D. Electroporation for DNA immunization: Clinical application. *Expert Rev. Vaccines* **9,** 503–517 (2010).
34. Sallusto, F., Geginat, J. & Lanzavecchia, A. Central memory and effector memory T cell subsets: Function, generation, and maintenance. *Annu. Rev. Immunol.* **22,** 745–763 (2004).
35. Greenland, J. R. *et al.* β-amino ester polymers facilitate *in vivo* DNA transfection and adjuvant plasmid DNA immunization. *Mol. Ther.* **12,** 164–170 (2005).
36. Saade, F. & Petrovsky, N. Technologies for enhanced efficacy of DNA vaccines. *Expert Rev. Vaccines* **11,** 189–209 (2012).
37. Sullivan, S. P. *et al.* Dissolving polymer microneedle patches for influenza vaccination. *Nature Med.* **16,** 915–920 (2009).
38. Zhu, Q. *et al.* Immunization by vaccine-coated microneedle arrays protects against lethal influenza virus challenge. *Proc. Natl Acad. Sci. USA* **106,** 7968–7973 (2009).
39. Chen, X. *et al.* Improved DNA vaccination by skin-targeted delivery using dry-coated densely-packed microprojection arrays. *J. Controlled Release* **148,** 327–333 (2010).
40. Gill, H. S., Soederholm, J., Prausnitz, M. R. & Saellberg, M. Cutaneous vaccination using microneedles coated with hepatitis C DNA vaccine. *Gene Ther.* **17,** 811–814 (2010).
41. Mikszta, J. A. *et al.* Improved genetic immunization via micromechanical disruption of skin-barrier function and targeted epidermal delivery. *Nature Med.* **8,** 415–419 (2002).
42. Song, J-M. *et al.* DNA vaccination in the skin using microneedles improves protection against influenza. *Mol. Ther.* **20,** 1472–1480 (2012).
43. Verstrepen, B. E. *et al.* Improved HIV-1 specific T-cell responses by short-interval DNA tattooing as compared to intramuscular immunization in non-human primates. *Vaccine* **26,** 3346–3351 (2008).
44. Denet, A-R., Vanbever, R. & Preat, V. Skin electroporation for transdermal and topical delivery. *Adv. Drug Deliv. Rev.* **56,** 659–674 (2004).
45. Wallace, M. *et al.* Tolerability of two sequential electroporation treatments using MedPulser DNA Delivery System (DDS) in healthy adults. *Mol. Ther.* **17,** 922–928 (2009).
46. Boudou, T., Crouzier, T., Ren, K., Blin, G. & Picart, C. Multiple functionalities of polyelectrolyte multilayer films: New biomedical applications. *Adv. Mater.* **22,** 441–467 (2010).

47. Dimitrova, M. *et al.* Sustained delivery of siRNAs targeting viral infection by cell-degradable multilayered polyelectrolyte films. *Proc. Natl Acad. Sci. USA* **105,** 16320–16325 (2008).
48. Jessel, N. *et al.* Multiple and time-scheduled *in situ* DNA delivery mediated by β^2-cyclodextrin embedded in a polyelectrolyte multilayer. *Proc. Natl Acad. Sci. USA* **103,** 8618–8621 (2006).
49. Kim, B-S., Park, S. W. & Hammond, P. T. Hydrogen-bonding layer-by-layer-assembled biodegradable polymeric micelles as drug delivery vehicles from surfaces. *ACS Nano* **2,** 386–392 (2008).
50. Kim, B-S., Smith, R. C., Poon, Z. & Hammond, P. T. MAD (multiagent delivery) nanolayer: Delivering multiple therapeutics from hierarchically assembled surface coatings. *Langmuir* **25,** 14086–14092 (2009).
51. Lynn, D. M. Peeling back the layers: Controlled erosion and triggered disassembly of multilayered polyelectrolyte thin films. *Adv. Mater.* **19,** 4118–4130 (2007).
52. Akinc, A., Anderson, D. G., Lynn, D. M. & Langer, R. Synthesis of poly(β-amino ester)s optimized for highly effective gene delivery. *Bioconjug. Chem.* **14,** 979–988 (2003).
53. Stoitzner, P. *et al.* Migration of Langerhans cells and dermal dendritic cells in skin organ cultures: Augmentation by TNF-α and IL-1β. *J. Leukoc. Biol.* **66,** 462–470 (1999).

Acknowledgements

This work was supported in part by the Ragon Institute of MGH, MIT, and Harvard, the NIH (AI095109), and the Institute for Soldier Nanotechnology (Dept. of Defense contracts W911NF-07-D-0004 and W911NF-07-0004, T.O. 8). We thank R. Parkhill and M. Nguyen (VaxDesign) for assistance with microneedle array fabrication. D.J.I. is an investigator of the Howard Hughes Medical Institute.

Author contributions

P.C.D., P.T.H. and D.J.I. designed the experiments. P.C.D., D.H.B. and D.J.I. designed macaque skin studies. P.C.D. carried out the experiments; Y.M. performed *in vitro* nucleic acid release studies. B.H. synthesized the PNMP polymers. A.D.M. and J.A.K. collected the macaque skin. P.C.D., P.T.H. and D.J.I. analysed the data and wrote the paper.

Additional information

Supplementary information is available in the online version of the paper. Reprints and permissions information is available online at www.nature.com/reprints. Correspondence and requests for materials should be addressed to P.T.H or D.J.I.

Competing financial interests

The authors declare no competing financial interests.